Nuclear Instruments and Methods in Physics Research B 269 (2011) 2307–2311

Contents lists available at ScienceDirect

Nuclear Instruments and Methods in Physics Research B

journal homepage: www.elsevier.com/locate/nimb

Stopping power and ranges of electrons, protons and alpha particles in liquid water using the Geant4-DNA package

Z. Francis [a,*], S. Incerti [b], M. Karamitros [b], H.N. Tran [b], C. Villagrasa [a]

[a] Institut de Radioprotection et de Sûreté Nucléaire, DRPH/SDE, Avenue de la division Leclerc, 92262 Fontenay-aux-Roses Cedex, France
[b] Université Bordeaux 1, CNRS/IN2P3, Centre d'Etudes Nucléaires de Bordeaux-Gradignan, CENBG, Chemin du solarium, BP 120, 33175 Gradignan, France

ARTICLE INFO

Article history:
Available online 26 February 2011

Keywords:
Monte-Carlo
Geant4
Geant4-DNA
Stopping power
Ranges

ABSTRACT

This paper presents stopping power and ranges of electrons, protons, and alpha particles in liquid water, calculated using the latest Geant4-DNA processes implemented in the Geant4 Monte Carlo simulation toolkit. Inelastic cross sections are obtained using the first Born approximation and semi-empirical formulas like Rudd's model for ionisation and the Miller and Green formula for excitation. Elastic collisions and vibrational excitations are considered for tracking electrons until complete thermalisation (0.025 eV). A speed scaling procedure with an effective charge screening term was used to compute alpha particle and heavy ion cross sections. Geant4-DNA simulations were carried out using thin liquid water volumes to determine the linear energy loss (dE/dX), while larger volumes were used to obtain the particle range. While results converge for highly energetic particles, differences are observed for low energies when the applied theoretical models begin to diverge from each other. Results show a good agreement between the analytical calculations obtained from the models, the Geant4-DNA Monte Carlo simulation predictions and the data published in the ICRU reports. Geant4-DNA processes apply to the following energy ranges: 0.025 eV–1 MeV for electrons, 100 eV–100 MeV for protons and 1 keV–400 MeV for alpha particles in liquid water, however since experimental data for very low energies is scarce and very difficult to obtain these processes could not be thoroughly validated so they are recommended for energies above 1 eV for electrons, 1 keV for protons and 10 keV for alpha particles. Relativistic, highly charged ions were implemented in our own "house" version of the code and will be available in future releases of Geant4.

1. Introduction

Remaining a cheap but effective way to study track structure and energy deposits in matter, Monte Carlo codes have noticeably evolved over the last 10 years. In this paper we present the recently improved Geant4-DNA package [1–3], an extension to the free open source Geant4 Monte Carlo toolkit [4,5]. The extended processes can generate ionising tracks for microdosimetry applications, and they are partially available for download with the Geant4 toolkit from the official Geant4 webpage. The entire package will be available in future releases, once the required testing procedures are complete (December 2010). The physics processes are dedicated to sub-cellular studies. Specific cross sections were calculated for protons, electrons and alpha particles, taking into consideration all possible interactions such as ionisation, excitation, charge transfer and elastic scattering. Inelastic cross sections were calculated using the first Born approximation. For low energies, corrections were used for electrons, and semi-empirical models replaced the theoretical calculations for protons and alpha particles in liquid water. Processes are available for protons between 100 eV–100 MeV (recommended above 1 keV), relativistic electrons up to 1 MeV, sub-excitation electrons until complete thermalisation at 0.025 eV (recommended down to 1 eV) and alpha particles between 1 keV–400 MeV (recommended above 10 keV), using the Rudd ionisation model and the Miller and Green model for excitation. Carbon ions and high energy alphas (1 MeV/amu–10 GeV/amu) were implemented in a "house" version for testing and validation.

This work is primarily dedicated to applications in radiobiology. One major parameter characterising radiation in this field is the Linear Energy Transfer (LET). Also referred to as stopping power, it represents the mean amount of energy an incident particle transfers to the target medium per unit path length. Furthermore, most of the energy is deposited through the secondary electrons that are produced by the ion's interactions with the target's molecules. The shape of the radial energy deposition around the ion track will depend on the secondary electrons energies and ranges. It is therefore important to characterise the extended processes for studying the

* Corresponding author.
E-mail address: ziad.francis@gmail.com (Z. Francis).

0168-583X/$ - see front matter © 2011 Elsevier B.V. All rights reserved.
doi:10.1016/j.nimb.2011.02.031

estimated LET and particle ranges that can be deduced from the code. Simulations are carried out using the Geant4-DNA package, which estimates the ranges and LET of different particles (alphas, protons and electrons) with different kinetic energies. The obtained results are compared to theoretical calculated values and recommended data, including the ICRU reports.

2. The GEANT4-DNA physics

Ionisation and excitation inelastic cross-sections were calculated using the Plane-Wave First Born Approximation (FBA). Detailed by Landau and Lifshitz [6] and Bethe [7,8], it is now widely used to calculate inelastic data, which is a main prerequisite for Monte Carlo transport codes. In our case, because water is considered to be the major component of biological tissue, the cross sections mentioned hereafter are related only to liquid water. We considered 5 ionisation states and 5 excitation states for the water molecule, using the latest dispersion model described by Emfietzoglou et al. [9]. Cross sections described by Dingfelder et al. [10,11] are also available as an alternative data set. In short, the dielectric-response function (DRF) of the target molecule is used to calculate the interaction cross sections for incident particles. According to the FBA, energy and momentum transfers are related to the energy loss function (ELF) $\mathrm{Im}[-1/\varepsilon(E,q)]$, where ε is the complex DRF characterising the target molecule [6]. A short summary shall be presented here; for calculation details refer to [12–19] and [10,11]. The Born double differential inverse mean-free-path (IMFP) is given in terms of energy loss E and momentum transfer q by:

$$\frac{d^2\Sigma(T,E,q)}{dE\cdot dq}=\frac{1}{\pi\cdot\alpha_0\cdot T\cdot q}\mathrm{Im}\left[\frac{-1}{\varepsilon(E,q)}\right]\theta[q-q_-(E,\tau)]\theta[q_+(E,\tau)-q]\theta[\tau-E] \tag{1}$$

where α_0 is the Bohr radius, τ is the particle kinetic energy, $T=(m/M)\tau$ is the kinetic energy of an electron travelling with the same velocity of the considered particle, m is the electron mass, M is the particle mass, θ is the Heaviside step function and $\varepsilon=\varepsilon_1+i\varepsilon_2$ represents the complex dielectric-response function of the target material. The momentum transfer limits are given as follows:

$$q_\pm=\sqrt{2M}(\sqrt{\tau}\pm\sqrt{\tau-E}) \tag{2}$$

The single differential cross section and the integrated IMFP can be obtained simply by the following expressions:

$$\frac{d\Sigma(T,E)}{dE}=\int\frac{d^2\Sigma(T,E,q)}{dE.dq}.dq \tag{3}$$

$$\Sigma(T)=\int dE\int\frac{d^2\Sigma(T,E,q)}{dE.dq}dq \tag{4}$$

However, the most important task in such calculations is the determination of the ELF, also called the "Bethe surface" of the target. This term characterising the medium was thoroughly studied in the literature and also by D. Emfietzoglou for water in its three different phases. The first step is to fit the experimental points of the DRF in the optical limit range ($q=0$) into a series of Drude equations and then apply the dispersion model for the positive momentum transfer range ($q>0$). The only available experiments measuring the ELF of water molecules in the optical limit range were reported by Hayashi et al. [20] and Heller et al. [21].

For low energies, when the incident particle speed approaches the speed of electrons orbiting the target molecule (<1 keV for electrons and <300 keV for protons), the FBA is no longer applicable on its own. In this case, for protons, cross sections were calculated using a combination of semi-empirical models like the Rudd formula for ionisation [22,23] and the Miller and Green formula for excitation [11]. For electron ionisation, the FBA is corrected using the exchange term proposed in ICRU report 37 [24] and a simple coulomb field correction, which accounts for the potential energy gained by the incident electron in the field of the target molecule [25]. The cross section for a given energy T is then calculated for an increased value $T'=T+B_j+U_j$ for ionisation, where B_j and U_j are the j^{th} shell binding energy and the electron average kinetic energy on this shell. For excitation: $T'=T+2E_j$, where E_j is the j^{th} excitation energy. Electron propagation is highly governed by elastic scattering, especially at low energies where this process dominates and a particle goes through a series of scatters without losing energy before an inelastic interaction occurs. Elastic collisions are described by two alternative models; the screened Rutherford and the Champion models [26].

In theory, electrons below 8 eV cannot ionise a water molecule, as this energy is lower than the least bounded shell in the target, so they are called sub-excitation electrons. These electrons can still undergo vibrational and rotational excitations and elastic collisions until complete thermalisation (0.025 eV). Lacking a theory that describes accurately such phenomena, experimental cross sections published by Michaud et al. [27] for ice targets were used after a phase-scaling procedure to account for the liquid phase of the molecules [28]. Electron attachment can also occur between ~8–13 eV. Here we have used the experimental results reported by Melton [29]. For electrons of energy exceeding 10 keV, relativistic assumptions are considered. Longitudinal as well as transverse interactions are taken into consideration. The total ionisation cross section is then given by Bousis et al. [30]:

$$\Sigma_j=\Sigma_j^L+\Sigma_j^T \tag{5}$$

where

$$\Sigma_j^L=\frac{2}{\pi\alpha_0\beta^2(T)mc^2}\left\{\int_{E\min}^{E\max}dE\int_{k\min}^{k\max}\mathrm{Im}\left[-\frac{1}{\varepsilon(E,k)}\right]_j\frac{dk}{k}\right\} \tag{6}$$

and

$$\Sigma_j^T=\frac{1}{\pi\alpha_0\beta^2(T)mc^2}\left\{\int_{E\min}^{E\max}\mathrm{Im}\left[-\frac{1}{\varepsilon(E,0)}\right]_j dE\right\}\times\left[\ln\left(\frac{1}{1-\beta^2(T)}\right)-\beta^2(T)\right] \tag{7}$$

mc^2 is the electron rest energy and $\beta=\frac{v}{c}$ is the ratio of the incident velocity to the velocity of light. The momentum transfer limits are $k_{\max,\min}=(c\hbar)^{-1}(\sqrt{T(T+2mc^2)})\pm\sqrt{(T-E)(T-E+2mc^2)}$, $E_{\min}$ is equal to the binding energy of each shell, and $E_{\max}=(T+B_j)/2$.

In addition to ionisation and excitation, the charge transfer process becomes dominant for low proton energies. It occurs when the incident proton captures an electron and becomes a neutral hydrogen atom by ionising a water molecule. The hydrogen can produce ionisations in the medium and can also undergo a stripping process, losing its orbital electron and returning to its ion state. In this case the electron is ejected in the projectile's direction with the same velocity; in this work excitations by hydrogen atoms have been neglected. Proton charge transfer and stripping processes are studied using semi-empirical formulas [11], and hydrogen atoms were tracked using the Rudd model with a term accounting for the screening effect caused by the projectile bound electron.

For alpha particles and heavier ions such as carbon and oxygen, a speed-scaling procedure was adopted using the proton cross sections, assuming that two particles with the same speed have the same cross section multiplied by an effective charge term. The effective charge and electron transfer for alpha particles were modelled using Dingfelder's approach [31,32]:

$$\frac{d\sigma_{\text{ion}}}{dE.dq}(v) = Z_{eff}^2(E)\frac{d\sigma_{\text{proton}}}{dE.dq}d(v) \quad (8)$$

where v is the projectile velocity and Z_{eff}^2 is the squared effective charge of the incident ion.

The use of an effective charge takes into account the screening effect of the nuclear charge caused by the boundary electrons of the incident particle. It depends on the energy transfer during the collision. A relatively recent model was concluded by Dingfelder [32], based on the work by Toburen et al. [33] and the model proposed by McGuire et al. [34]. This model describes the effective charge variation for He^0, He^+ and He^{++} projectiles. Charge transfer processes were calculated in the same way as for protons, by fitting an analytical formula to available experimental data.

For ions heavier than alphas, it is complicated to calculate cross sections for every single charge state of the particle. Thus a global effective charge, including the charge change effect as well as the charge screening for the incident ion, is used. The effective charge expression of Booth and Grant [35] is applied, given by the following expression:

$$Z_{eff}/Z = 1 - \exp(-1.316x + 0.112x^2 - 0.0650x^3) \quad (9)$$

where $x = 100\beta Z^{-2/3}$.

3. Results and discussion

Simulations are carried out by shooting particle beams through thin water slices and calculating the energy loss per unit path length (LET), while larger water volumes of full particle containment are used to obtain the particle range. Generally, most of the data in the literature are in good agreement for high incident energies (above 1 keV for electrons and 500 keV for protons). This is due to the common use of theoretical approximations like the FBA which converges accurately with the experimental data for high energies. In the low energy domain, calculations become more complicated, and one must use an alternative to the theoretical model. Most of the time, a semi-empirical formula of the user's choice is applied, which can explain the differences in the results. In the following, we will mostly concentrate on the low energy part of the results, as they remain important for radiobiology, especially in the Bragg peak region.

For the stopping power simulations, the thickness of the target is sufficiently small, so there is no important change in the incident particle's energy when crossing the medium. It is also thick enough to allow more than a minimum of 10 interactions for each particle. After thorough trials, we took targets allowing 5% of maximum energy loss for ions and high energy electrons. When the energy of the particle crossing the target drops below 95% of its initial energy, it is stopped and the energy loss is divided by its track length. This is not valid for low energy electrons since an electron of less than 50 eV, for example, can lose its energy in one or two steps. This is technically cumbersome, leading to inaccurate results since the energy of the electron is changing relatively quickly. In this case, the stopping power was calculated analytically from the cross sections that are included in Geant4-DNA.

For the calculation of ranges target dimensions should be large enough to allow the particle to come to a full stop within the water volume. Here we can distinguish "the track length", which corresponds to the total length of the path followed by the particle including the direction changes, from "the range" which is the radius vector between the starting point and the stopping point, and "the projected range" which corresponds to the penetration depth in the target. For ions, the track length and the range are almost the same, since the direction change is neglected. This is not true though in the case of electrons where direction changes occur frequently due to elastic collisions. This is reflected in Fig. 2, where

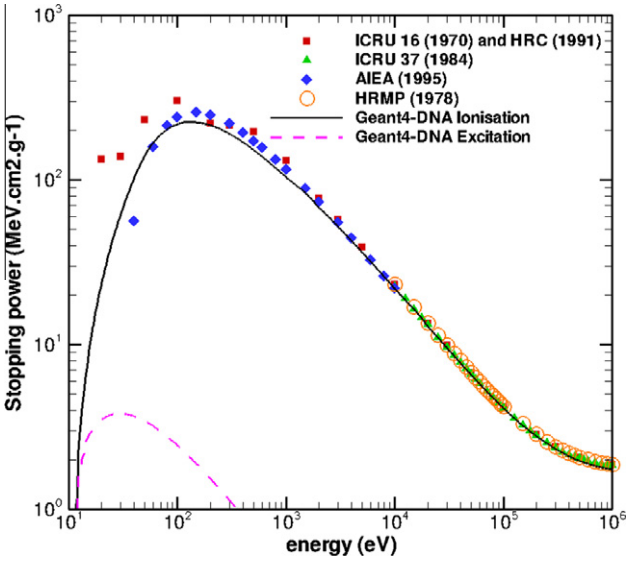

Fig. 1. Electron stopping power in liquid water calculated using Geant4-DNA and compared to recommended data [36–38] and to the values published in the ICRU reports 16 and 37 [39,24].

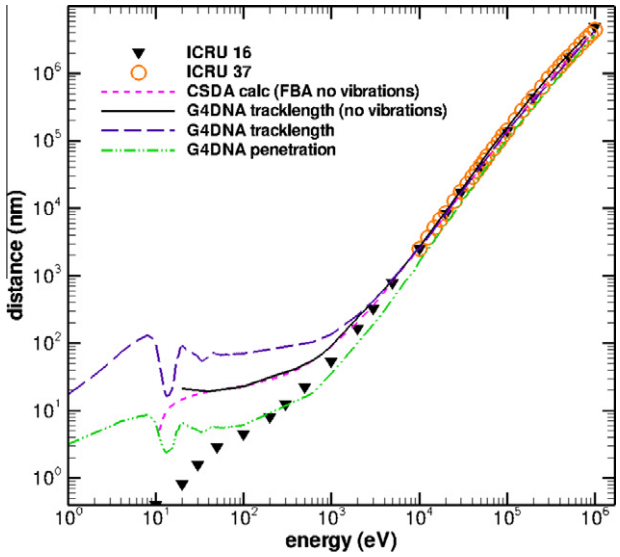

Fig. 2. Simulated electron ranges in water obtained with and without the vibrational excitation process and compared to the CSDA (see text) calculations and to the ranges published in the ICRU reports 16 [39] and 37 [24].

the difference between the penetration of a normal incident electron on the target surface and its track length inside the volume is clearly visible below a certain energy level (~10 keV).

Fig. 1 shows the electrons stopping power in liquid water. One can notice that the excitation contribution is very small and appears only in the low energies, although this process may still contribute across the whole energy range. The obtained results are compared to recommended data [36–38] and the values published in ICRU reports 16 and 37 [39,24]. A satisfying agreement is obtained for high incident energies above 150–200 eV, whereas differences increase for lower energies. In fact, electron cross sections below 50 eV are still a field of study where experiments are difficult to carry out and there is no evident theory leading to accurate results. For this reason, we consider these results satisfying for our Monte Carlo study.

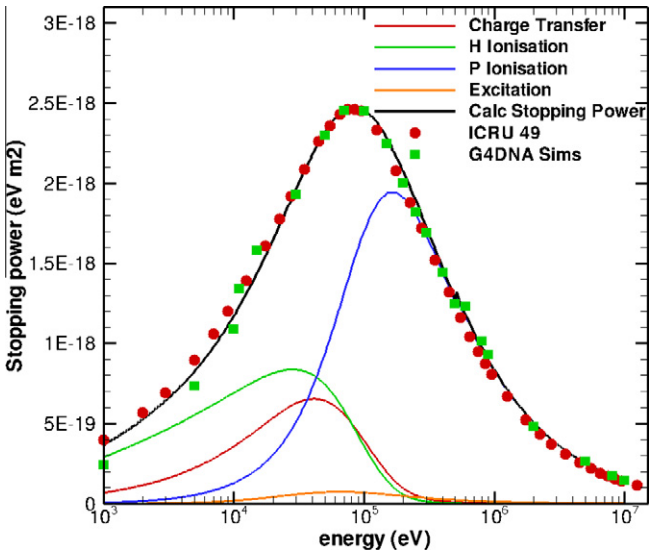

Fig. 3. Proton stopping power contributions of the different interacting processes. The calculated total curve (full line) is compared with the results of the simulation (squares) and the ICRU report 49 [40] values.

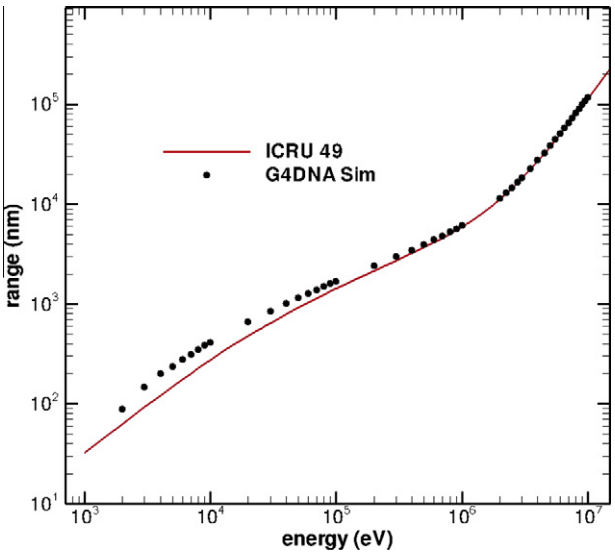

Fig. 5. Simulated alpha particles ranges in liquid water compared to ICRU 49 [40] values.

Ranges of electrons versus kinetic energy are shown in Fig. 2. The results obtained using Geant4-DNA processes are compared to ranges published in ICRU reports 37 [24] and 16 [39] and to the continuous slowing down approximation (CSDA) range calculated using the cross sections from the FBA. The oscillations are due to quickly decreasing cross sections at low energies for the different inelastic shells interactions. The projected range is also shown. A general agreement is observed for high energies, while low energy experimental data are unfortunately hard to find for liquid water.

Fig. 3 shows the contribution of the different processes to proton stopping power. Above 1 MeV, ionisation is the only dominating interaction, while the excitation and the charge transfer process contribute significantly around 50 keV. Moreover, the contribution from hydrogen ionisation is also shown. Note that this result takes into account the charge state ratio as the proton switches between the hydrogen neutral state and the ionised state; the hydrogen stopping power here is multiplied by the probability that the particle will be in the neutral charge state. Below 10 keV the calculated total stopping power is lower than ICRU values, as are the simulation results. Although the difference does not seem great, at these energies nuclear collisions can contribute up to 24% to the stopping power (see ICRU 16 [39]) of protons below 5 keV in water. Nuclear collisions were neglected in our case, so the processes used are recommended for relatively high energies (above 5 keV). However, in radiobiology energies below 5 keV are not reached unless one aims to simulate the complete stop of the proton in biological matter. The effect of the stopping power differences is seen clearly in Fig. 4, where the protons ranges are presented versus their incident energies. Below about 100 keV the difference between the simulation and ICRU 16 and 49 values increases as energy decreases. This is probably due to the neglected nuclear collisions, as already mentioned, but it would be an interesting subject for future investigation if necessary. This same difference is also noticed for alpha particle ranges represented in Fig. 5. In both cases, the ranges are higher than ICRU standard values; obviously taking one more interaction into account will shorten the range, since this will increase the total cross section and decrease the mean free path of the particle.

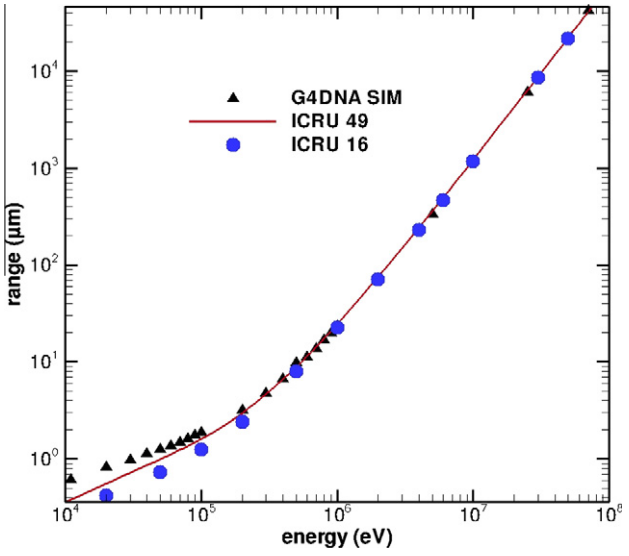

Fig. 4. Simulated proton ranges in liquid water compared to ICRU 16 [39] and 49 [40] published values.

4. Conclusion

In conclusion, we have presented a set of stopping powers and ranges of electrons, protons and alpha particles calculated in water using the Geant4-DNA package. The results show an overall agreement for high particle energies, in comparison with several data sources. Depending on the accuracy required, the user may limit his simulations to a minimum energy value. The described process package is useful for radiobiological applications, microdosimetry and track structure at the molecular level. Heavy ions (Carbon, Nitrogen and Oxygen) electromagnetic processes including ionisation and excitation interactions are under development and will be available soon, as part of the whole Geant4-DNA package described in this paper, to be publicly released in December 2010. Extensions regarding nuclear collisions at low energies are required for improving the toolkit's accuracy for ion simulations.

References

[1] S. Incerti et al., The Geant4-DNA project, Int. J. Mod. Sim. Sci. Com. 1 (2) (2010) 157.
[2] S. Chauvie, Z. Francis, S. Guatelli, S. Incerti, B. Mascialino, G. Montarou, P. Moretto, P. Nieminen, M.G. Pia, Rad. Res. 166 (4) (2006) 676–677.
[3] S. Incerti, A. Ivanchenko, M. Karamitros, A. Mantero, P. Moretto, H.N. Tran, B. Mascialino, C. Champion, V.N. Ivanchenko, M.A. Bernal, Z. Francis, C. Villagrasa, G. Baldacchino, P. Gueye, R. Capra, P. Nieminen, C. Zacharatou, Med. Phys. 37 (2010) 4692–4708.
[4] S. Agostinelli et al., Nucl. Instr. and Meth. A 506 (2003) 250–303.
[5] J. Allison et al., IEEE Trans. Nucl. Sci. 53 (1) (2006) 270–278.
[6] Landau, Lifshitz, Electrodynamics of Continuous Media, 2nd edition, Elsevier (2009).
[7] H. Bethe, Ann. Phys. (Leipzig) 5 (1930) 325–400.
[8] H. Bethe, H. In Geiger, K. Scheel (Eds.), Handbuch der Physik, Vol 24/1, Springer, Berlin, 1933. p. 273.
[9] D. Emfietzoglou, H. Nikjoo, Rad. Res. 167 (2007) 110–120.
[10] M. Dingfelder, D. Hantke, M. Inokuti, H.G. Paretzke, Rad. Phys. and Chem. 53 (1998) 1–18.
[11] M. Dingfelder, D. Hantke, M. Inokuti, H.G. Paretzke, Rad. Phys. and Chem. 59 (255–275) (2000) 1–18.
[12] D. Emfietzoglou, K. Karava, G. Papamichael, M. Moscovitch, Phys. Med. Biol. 48 (2003) 2355–2371.
[13] D. Emfietzoglou, Rad. Phys. Chem. 66 (2003) 373–385.
[14] D. Emfietzoglou, M. Moscovitch, A. Pathak, Nucl. Instr. and Meth. B 212 (2003) 101–109.
[15] D. Emfietzoglou, M. Moscovitch, Nucl. Instr. and Meth. B 209 (2003) 239–245.
[16] D. Emfietzoglou, A. Pathak, M. Moscovitch, Nucl. Instr. and Meth. B 230 (2005) 77–84.
[17] D. Emfietzoglou, F. Cucinotta, H. Nikjoo, Rad. Res. 164 (2005) 202–211.
[18] D. Emfietzoglou, H. Nikjoo, Rad. Res. 163 (2005) 98–111.
[19] D. Emfietzoglou, H. Nikjoo, A. Pathak, Nucl. Instr. and Meth. B 249 (2006) 26–28.
[20] H. Hayashi, N. Watanabe, Y.J. Udagawa, Chem. Phys. 108 (1998) 823–825.
[21] J.M. Heller, R.N. Hamm, R.D. Birkhoff, L.R. Painter, J. Chem. Phys. 60 (1974) 3483–3486.
[22] M.E. Rudd, Y.-K. Kim, D.H. Madison, T.J. Gay, Rev. Mod. Phys. 64 (1992) 441–490.
[23] M.E. Rudd, Y.-K. Kim, D.H. Madison, J.W. Gallagher, Rev. Mod. Phys. 57 (1985) 965–994.
[24] ICRU report 37, International Commission on Radiation Units and Measurements, Bethesda, Maryland, USA, 1984.
[25] L. Vriens, Phys. Rev. 141 (1) (1966) 88–92.
[26] C. Champion, S. Incerti, H. Aouchiche, D. Oubaziz, Rad. Phys. Chem. 78 (2009). 745–750.
[27] M. Michaud, A. Wen, L. Sanche, Rad. Res. 159 (2003) 3–22.
[28] J. Meesungnoen, J.P. Jay-Gerin, A. Filali-Mouhim, S. Mankhetkorn, Rad. Res. 158 (2002) 657–660.
[29] E.C. Melton, J. Chem. Phys. 57 (10) (1972) 4218.
[30] C. Bousis, D. Emfietzoglou, P. Hadjidoukas, H. Nikjoo, A. Pathak, Nucl. Instr. and Meth. B 266 (2008) 1185–1192.
[31] M. Dingfelder, Rad. Prot. Dosim. 99 (1–4) (2002) 23–28.
[32] M. Dingfelder, L.H. Toburen, H.G. Paretzke, The Monte Carlo Method: Versatility Unbounded in a Dynamic Computing World Chattanooga, Tennessee, April 17-21, American Nuclear Society, LaGrange Park, IL, 2005.
[33] L.H. Toburen, N. Stolterfoht, P. Zienn, Schneider, Phys. Rev. A 24 (1981) 1741–1745.
[34] J.H. McGuire, N. Stolterfoht, P.R. Simony, Phys. Rev. A 24 (1981) 97–102.
[35] W. Booth, I.S. Grant, Nucl. Phys. 63 (1965) 481.
[36] Y. Tabata, Y. Ito, S. Tagawa, Handbook of Radiation Chemistry, CRC Press, Boca Raton, Florida, USA, 1991.
[37] A. Brodsky, Physical science and engineering data, Handbook of Radiation Measurement and Protection, CRC Press, West Palm Beach, Florida, USA, 1978.
[38] H. Paul, M.J. Berger, Atomic and Molecular Data for Radiotherapy and Radiation Research, IAEA-ECDOC-799, International Atomic Energy Agency, Vienna, 1995. pp. 415–545.
[39] ICRU report 16, International Commission on Radiation Units and Measurements, Washington DC, USA, 1970.
[40] ICRU report 49, International Commission on Radiation Units and Measurements, Bethesda, Maryland, USA, 1993.